Mechanical and electrical properties of polyacetylene films oriented by tensile drawing

Yong Cao, Paul Smith*† and Alan J. Heeger‡§
*Institute for Polymers and Organic Solids, *Materials Department, †Department of Chemical and Nuclear Engineering, and ‡Physics Department, University of California at Santa Barbara, Santa Barbara, CA 93106, USA*
(Received 5 March 1990; accepted 17 April 1990)

An improved technique was developed for tensile drawing of polyacetylene films prepared by the non-solvent polymerization method of Akagi *et al.*; draw ratios as high as 15 were obtained. Tensile drawing and the associated orientation resulted in major improvement of both the mechanical properties and the electrical conductivity (after doping). Maximum values for the modulus and tensile strength were 50 GPa and 0.9 GPa, respectively. The electrical conductivities of highly drawn thin films, doped with iodine, along the orientation direction reached values at room temperature of up to 3×10^4 S cm^{-1}, with an anisotropy, $\sigma_{\parallel}/\sigma_{\perp} > 250$. Both Young's modulus and the tenacity decreased upon doping, typically by a factor of about 4–5, which is indicative of reduced intersegmental interaction. The results demonstrate that the electrical conductivity increases linearly with the modulus and tensile strength, with polymer chain orientation as the implicit variable.

(Keywords: mechanical properties; electrical properties; polyacetylene films; tensile drawing)

INTRODUCTION

Polyacetylene has been of special interest as the prototypical conducting polymer since the discovery in 1977[1] that the electrical conductivity of conjugated polymers can be controlled over the full range from insulator to metal through charge transfer doping. Recent studies[2–4] demonstrated that major improvements in solid-state properties can be achieved with higher-quality polyacetylene obtained through improved synthesis and processing. Refinement of the polymerization by thermal pretreatment of the Ziegler–Natta catalyst results in polyacetylene film which can be stretched to higher draw ratios; these more highly oriented films exhibit higher electrical conductivity[3,4] and significantly improved mechanical properties[4,5].

In this paper, we describe an improved method for tensile drawing of polyacetylene films (prepared by non-solvent polymerization using a thermally pretreated variation of the Shirakawa catalyst) after equilibration in certain organic liquids, which serve as plasticizers in the deformation process. The maximum draw ratio (λ) achieved was $\lambda_{max} = 15$. The mechanical and electrical properties of such highly drawn polyacetylene films were measured before and after doping. The results are presented and discussed in the context of the degree of structural order as inferred from wide-angle X-ray diffraction (WAXD) patterns. The data demonstrate that the electrical conductivity increases linearly with the modulus and tensile strength, with chain orientation as the implicit variable. For polyacetylene films prepared in this way, the maximum values obtained were 50 GPa and 0.9 GPa for the modulus and tensile strength, respectively. Thin films doped with iodine exhibited electrical conductivities along the orientation direction (at room temperature) up to 3×10^4 S cm^{-1}, with an anisotropy, $\sigma_{\parallel}/\sigma_{\perp} > 250$. Both Young's modulus and the tenacity decreased upon doping, typically by a factor of about 4–5, which is explained in terms of reduced intersegmental interaction.

EXPERIMENTAL

Polymerization of acetylene

Polyacetylene films were prepared according to the non-solvent method recently described by Akagi *et al.*[4]. A standard $Ti(OBu)_4/AlEt_3$ catalyst was used; the concentration of catalyst was 0.5 mol l^{-1} of $Ti(OBu)_4$ in cumene, and the ratio Al to Ti was 2.0. After ageing at room temperature for 1 h, the catalyst solution was heated (with mild stirring) to 150°C under a flow of argon for 5 h. After cooling, the catalyst solution was transferred into the polymerization flask. The cumene was then pumped off at room temperature until the vapour pressure was below 5 mTorr. Polymerization was carried out at −78°C under an initial acetylene pressure of 600 Torr. The thickness of the resulting polyacetylene films was controlled by changing the thickness of the catalyst layer coated on the inner glass wall of the polymerization flask and by the polymerization time. Specifically, polyacetylene films with an *initial* thickness of 50–60 μm (hereafter designated as thick films) and 10–12 μm (hereafter designated as thin films) were prepared for deformation experiments and detailed characterization.

After completion of the polymerization, the polyacetylene films were held at −78°C and washed 20 times

§ To whom correspondence should be addressed
0032-3861/91/071210-09

with pure toluene trapped into the polymerization vessel from a side flask. The resulting films were stored in toluene at −78°C prior to tensile drawing.

Tensile drawing

After raising the container with polyacetylene films (in toluene) to room temperature, the polymer sample was removed and cut into 15 × 40 mm^2 specimens while still wet, in a dry-bag filled with argon. The cut samples were then quickly transferred into a flask containing an appropriate liquid to be used as a plasticizer (see the following section for details on the species used). The polyacetylene samples were stored in this liquid at −78°C overnight and allowed to come to equilibrium. After mounting a pre-cut, soaked polyacetylene film between two clamps, which were initially separated by 20 mm, the sample was manually stretched at room temperature using a simple apparatus for tensile drawing. The film was drawn under argon in a dry-bag to the desired draw ratio while still wet, and then pre-dried on the drawing apparatus under dynamic vacuum at room temperature overnight. After dismounting from the drawing apparatus, the films were once again dried under dynamic vacuum (less than 1 mTorr) for 48 h. The thicknesses after drawing to their maximum draw ratio were 25–30 μm for thick films and 3–5 μm for thin films (final widths about 3 mm). Isomerization of predominantly *cis*-polyacetylene films to the *trans*-$(CH{=}CH)_n$– configuration was accomplished by heating at 160°C and dynamic vacuum (less than 1 mTorr) for 30–40 min[6]. The samples were isomerized under stress (approximately 1×10^3 kg cm^{-2}) for additional stretching and to prevent shrinkage and/or curling.

Measurement of electrical and mechanical properties

Doping was carried out by exposing the polyacetylene films to I_2 vapour, or by exposing to various dopants in solution (using either I_2 in hexane, $FeCl_3$ in nitromethane, or $NOSbF_6$ in nitromethane). In all cases, the doping level was determined by weight uptake. The electrical conductivity was measured by the usual four-probe method. Film thicknesses were determined by optical microscopy, weight and/or with a micrometer.

Wide-angle X-ray diffraction patterns were recorded with a flat-film camera mounted on a Philips X-ray generator using Cu Kα radiation.

Stress–strain measurements were carried out at room temperature using an Instron tensile tester (model 1122) at a cross-head speed of 10 mm min^{-1}. Samples used in these measurements were 1–3 mm wide and the gauge length was 10 mm. Values of the tensile moduli reported in this paper refer to the initial or Young's modulus.

RESULTS AND DISCUSSION

Tensile drawing using organic liquids as plasticizers

Tensile drawing of the wet polyacetylene films yielded a maximum stretching ratio of about 15 for the thick films and about 10 for thin films. By contrast, fully dried polyacetylene films could not be extended beyond 6 times their original length under otherwise similar experimental conditions. Some variation in the maximum stretching ratio, λ_{max}, was found, dependent on the physicochemical characteristics of the liquid used as 'plasticizer'.

Table 1 Maximum draw ratio achieved for the thick polyacetylene films using different organic solvents as plasticizer

Solvent	Boiling point (°C)	Volume ratio	Maximum draw ratio[a]
Dried			6.0
1,5-Hexadiene	60	–	14.6
2,4-Hexadiene	82	–	14.0
1,7-Octadiene	114–121	–	12.3
Toluene	110.6	–	11.0
Cumene	152.0	–	9.5
Butylbenzene	183	–	8.5
Toluene/cumene		8/1	11.0
		4/1	15.2
		3/1	13.0
		2/1	10.0
Toluene/butylbenzene		8/1	13.0
		4/1	10.0

[a]Data before thermal isomerization

Specifically, it was observed that λ_{max} was dependent on the boiling point and the specific composition in the case of mixed liquids. The results are summarized in *Table 1*. The data in this table seem to indicate that λ_{max} is dependent on the relative content of solvent in the film and on the speed of evaporation of the solvent from the bulk of the film. Hexadienes, for example, were found to be excellent plasticizers for polyacetylene, presumably due to the easier penetration of these liquids into the polyacetylene lattice because of the similarity in molecular structures. Pure aromatic solvents appeared to be the least effective; however, a 4:1 mixture of toluene and cumene yielded excellent results. For thin films, the highest stretching ratio reached was $\lambda_{max} = 10$; we are inclined to attribute the thickness dependence of the maximum draw ratio to variation in the thickness of the thin films. Efforts to improve the uniformity (and thereby to increase λ_{max}) of thin polyacetylene films are in progress.

X-ray diffraction

The wide-angle X-ray diffraction patterns of drawn polyacetylene films show crystalline order with preferred orientation of the chain axis parallel to the stretching direction (see for example *Figure 1*); the (*hk*0) reflections are observed only with momentum transfer perpendicular to the stretching direction. The large number of equatorial reflections and off-axis reflections that can be seen in the diffraction patterns of *cis*-rich polyacetylene (*Figure 1a*) and *trans*-polyacetylene (*Figure 1b*) indicate a regular three-dimensional arrangement of the polymer chains. As compared with the *cis*-rich polyacetylene diffraction pattern (*Figure 1a*), *trans* –$(CH{=}CH)_n$– obtained by thermal isomerization yields a more clear fibre diffraction pattern (*Figure 1b*), implying improvement in the degree of structural order upon complete isomerization. The mosaic spread (derived from the half-width at half-maximum) is found to decrease to a value of about 3° as the draw ratio increases to $\lambda \geqslant 10$, comparable with that observed for polyacetylene prepared by the Durham method[7]. The strong small-angle reflections observed in the equatorial plane are connected with the long-range order transverse to the polyacetylene chain direction.

Assuming that the line broadening results from finite crystallite size, one can calculate the coherence length,

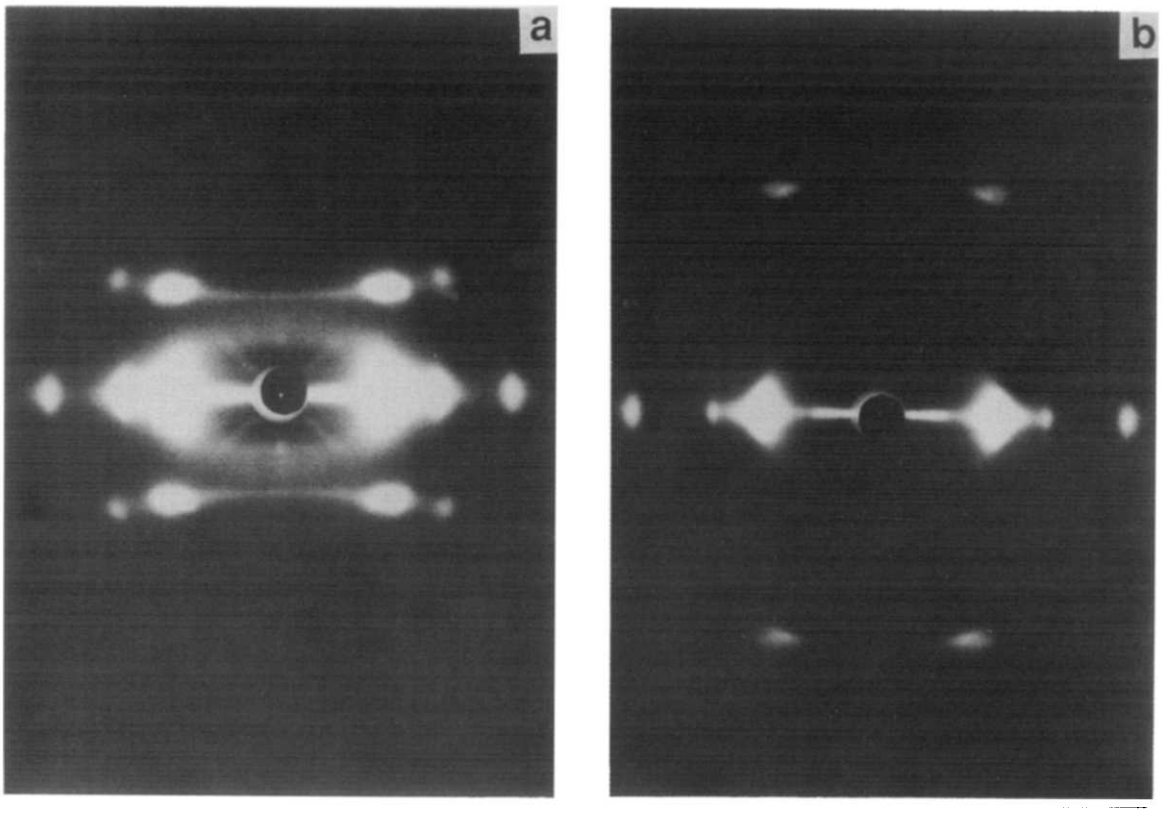

Figure 1 X-ray diffraction patterns of (a) *cis*-rich and (b) *trans*-polyacetylene films ($\lambda = 11$ for *cis* and $\lambda = 12$ for *trans* forms). Films were intentionally overexposed

ζ, from the Scherrer formula:

$$\zeta = 2\pi\lambda/\delta(2\theta) \quad (1)$$

where $\delta(2\theta)$ is the full width at half-maximum. We found $\zeta = 20$ nm for the order in the direction perpendicular to the chain direction for the highly drawn samples. This value is larger than that reported previously for *trans* $-(CH{=}CH)_n-$ prepared by the Durham method[7] by using a liquid-crystalline solvent in a magnetic field[8], or by the usual Shirakawa method[9] ($\zeta \sim 5$–10 nm). Comparing the diffraction patterns from samples with different draw ratios leads to the conclusion that the structural coherence length perpendicular to the draw direction increased somewhat (from approximately 10 nm at $\lambda = 4$ to approximately 20 nm at $\lambda = 15$) with increased orientation. This observation is of particular importance, for this indication of improved structure effectuated by tensile drawing demonstrates the positive effect of post-synthesis processing of polyacetylene on the molecular scale (in contrast to simple fibrillar alignment).

Figures 2 and *3* show the wide-angle X-ray diffraction patterns obtained from oriented polyacetylene films doped with iodine (*Figure 2a*), $NOSbF_6$ (*Figure 2b*) and $FeCl_3$ (*Figure 3*). The diffraction patterns indicate that the polyacetylene chain orientation remains essentially unchanged after doping. As observed in earlier studies[10], comparison of the fibre diffraction patterns of oriented *trans*-polyacetylene before and after doping shows that the principal equatorial reflections remain with only modest shifts in their positions as a result of lattice expansion to accommodate the dopant counterions. For all three dopants, there are sharp equatorial reflections (see *Table 2*) indicating an expansion of the unit cell due to intercalation of dopant molecules into the lattice of polyacetylene chains[11,12].

For the I_3-doped samples, the strong layer lines (*Figure 2a*) along the fibre orientation direction result from scattering from the counterions. Since these lines in the plane of the photograph indicate sheets of scattering rather than discrete reflections, it can be concluded that the I_3-counterions are arranged in columns in one-dimensional (1d) channels between the polyacetylene chains, with almost no phase coherence from column to column. For iodine doping, the diffraction patterns do not change with the doping level either in peak position or in the width of the streaks. Thus, the one-dimensional I_3-columns form essentially independently of one another. Shimamura *et al.*[13] observed (by electron diffraction) similar streaks on the meridian of very thin polyacetylene films polymerized epitaxially on dibromobenzene single crystals and lightly doped by iodine.

For SbF_6^-, the well defined features that appear in the diffraction pattern along the longitudinal direction (*Figure 2b*) are consistent with a structure in which the counterions are arranged in two-dimensional sheets, as proposed by Wiener *et al.*[14]. In contrast to these cases, the $FeCl_3$ doping yields extra reflections on the equator in addition to streaks in the meridian (*Figure 3a*). This seems to indicate the formation of a three-dimensional sublattice of $FeCl_4^-$ counterions. At increased $FeCl_4^-$ doping levels, the extra scattering from the counterions appears to be more isotropic, superposed on the anisotropic diffraction intensity from the partially oriented polyacetylene chains (*Figure 3b*).

We summarize the X-ray diffraction data for the three dopants in *Table 2*. In all three cases, we found evidence for the formation of a counteranion sublattice. Reflections on the meridian for $NOSbF_6$-doped polyacetylene can be assigned to overtones of the reflections at $1/d = 0.065$ Å^{-1}; thus, the repeat distance along the

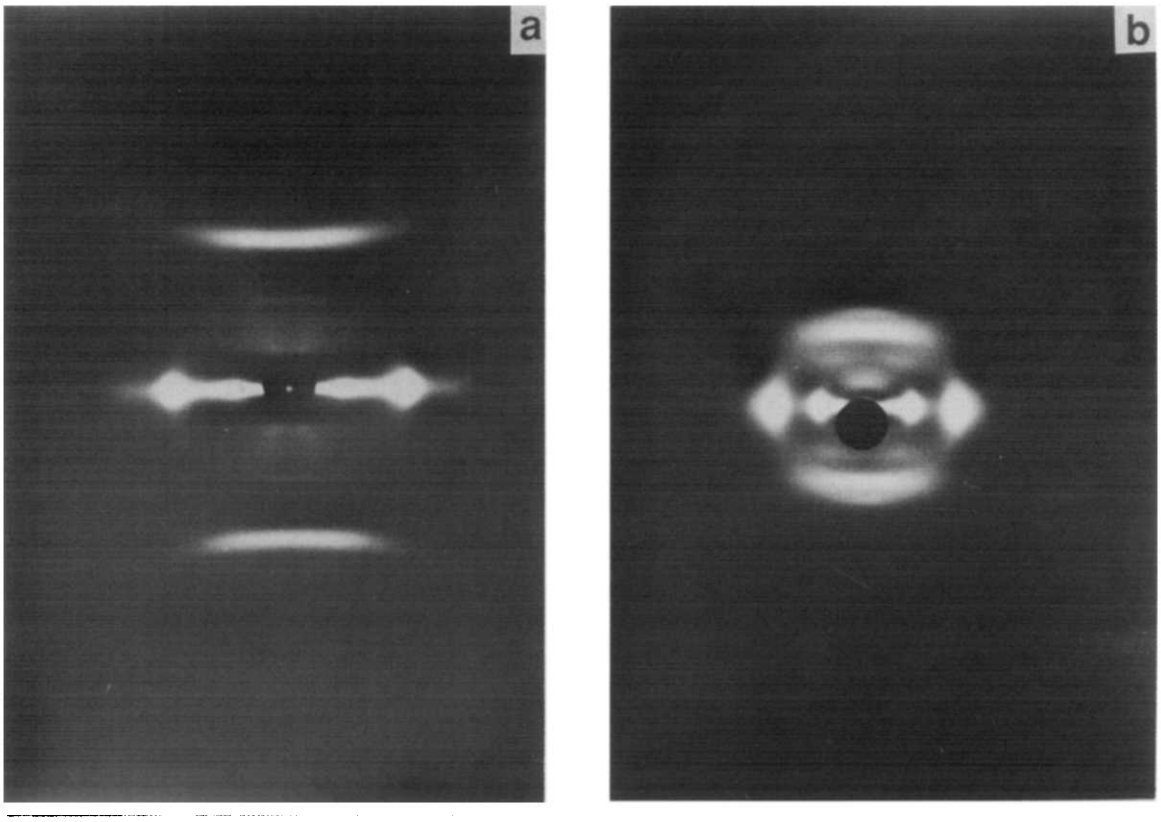

Figure 2 X-ray diffraction patterns of (a) iodine-doped ($y = 0.09$) and (b) $NOSbF_6$-doped ($y = 0.03$) polyacetylene films

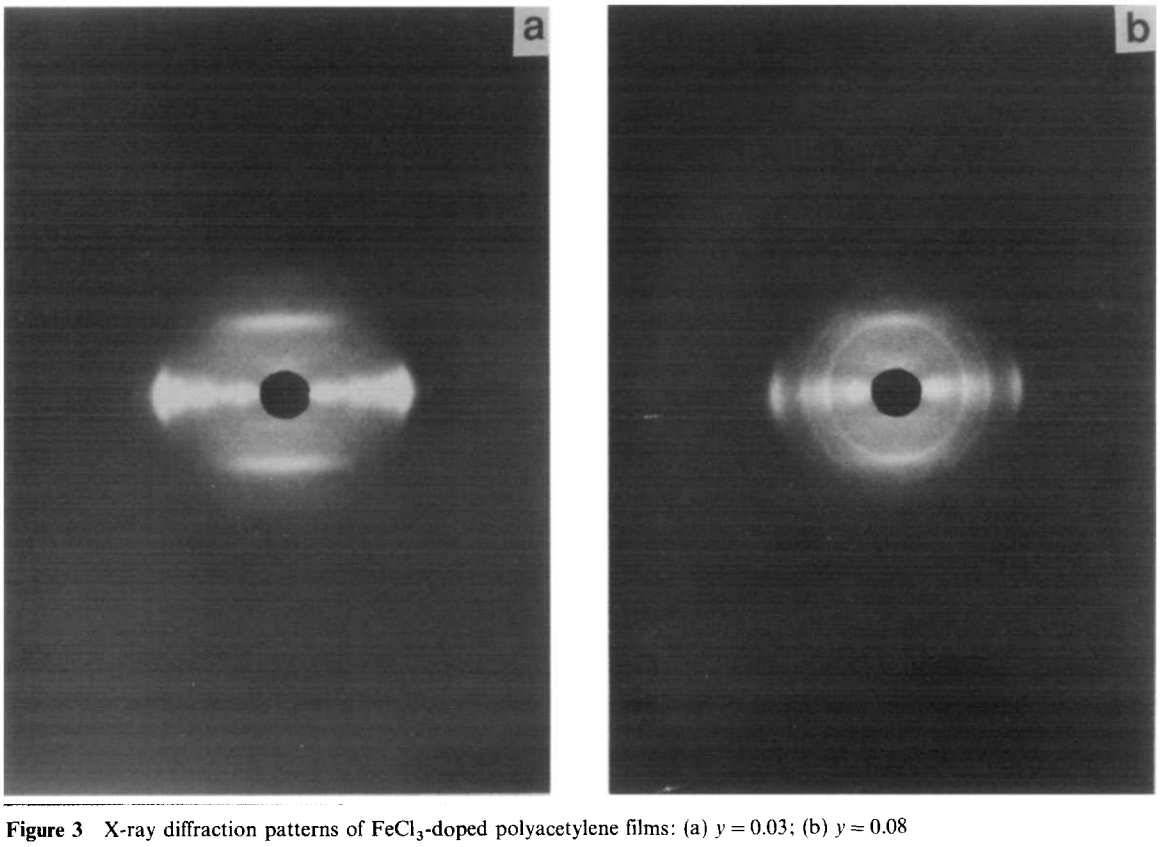

Figure 3 X-ray diffraction patterns of $FeCl_3$-doped polyacetylene films: (a) $y = 0.03$; (b) $y = 0.08$

stretching direction for the SbF_6^- lattice is 16.55 Å. For iodine-doped polyacetylene the reflections on the meridian cannot be assigned to the overtones of the reciprocal of 10.1 Å. Furthermore, the fact that the third reflection on the meridian at $d = 2.67$ Å is much more intense than the others seems to indicate that iodine atoms are located approximately uniformly along the counterion chain. Obviously, a more quantitative analysis of the diffraction patterns is needed to obtain more complete structural information.

Table 2 Wide-angle X-ray diffraction data for doped polyacetylene films

	Undoped			$(CH)(I_3^-)_{0.057}$			$(CH)(FeCl_4^-)_{0.033}$			$(CH)(SbF_6^-)_{0.078}$		
Reflections	d (Å)	$1/d$ ($Å^{-1}$)	Intensity	d (Å)	$1/d$ ($Å^{-1}$)	Intensity	d (Å)	$1/d$ ($Å^{-1}$)	Intensity	d (Å)	$1/d$ ($Å^{-1}$)	Intensity
Equatorial	3.69	(0.271)	vs	7.53	(0.133)	s	10.0	(0.1)	s	8.6	(0.116)	s
	3.23	(0.310)	w	3.53	(0.282)	vs	5.65	(0.177)	m	4.30	(0.233)	s
	2.58	(0.388)	s				5.02	(0.199)	w	3.62	(0.276)	w
	1.79	(0.559)	s				3.84	(0.260)	s			
	1.44	(0.694)	w				3.32	(0.301)	s			
							2.74	(0.365)	w			
Meridional				10.1	(0.0995)	m				16.44	(0.065)	w
										8.22	(0.122)	w
				4.48	(0.223)	w	5.65	(0.176)	s	5.48	(0.182)	s
				2.66	(0.375)	s	3.62	(0.276)	w	4.30	(0.233)	w

Mechanical properties

Figures 4 and *5* show the experimental values of the Young's modulus (*Figure 4*) and the tensile strength (*Figure 5*), respectively, for thick films of *undoped trans*-polyacetylene as a function of draw ratio (all samples were derived from the same polymerization batch). Although there is some scatter in the data, the modulus and tenacity increase approximately linearly with the draw ratio, as is commonly observed for most polymers drawn to moderate draw ratios. The modulus and tensile strength of *trans*-polyacetylene films stretched up to 15 times are 50 GPa and 0.9 GPa, respectively. These values are essentially equivalent to those observed for ultra-high-molecular-weight polyethylene[15] drawn to the same draw ratio. Recently, Akagi *et al.*[4] reported remarkable mechanical properties for drawn polyacetylene films prepared by non-solvent polymerization (100 GPa and 0.9 GPa for the modulus and tensile strength, respectively). We observed the same value for the tensile strength; however, we measured a significantly lower value for the Young's modulus (by about a factor of 2). The origin of difference in the modulus, unfortunately, is unknown.

An estimate of the modulus for perfectly oriented polyacetylene can be derived from the theoretical relation between the Young's modulus and draw ratio[16]:

$$E = [E_h^{-1} + (3\pi/4)\lambda^{-3/2}(E_u^{-1} - E_h^{-1})]^{-1} \quad (2)$$

where E is the measured modulus at a draw ratio of λ, E_h is the axial modulus of the perfectly oriented polymer, and E_u is the modulus of the unoriented polymer. The data for the *undoped* samples of *Figure 4* are plotted as E^{-1} *versus* $\lambda^{-3/2}$ in *Figure 6*. Although equation (2) was derived for tensile drawing of flexible chain polymers, the linear dependence observed in *Figure 6* appears to indicate that the complex deformation and isomerization of polyacetylene can be described with this relation despite the fact that these macromolecules are expected to be relatively stiff. Extrapolating to infinite draw ratio, i.e. $\lambda^{-3/2} \rightarrow 0$ (*Figure 6*), the axial modulus for perfectly oriented, *undoped* polyacetylene was estimated to be 290 ± 40 GPa. This value is consistent with that calculated for polyacetylene by Shimamura *et al.*[17] and Hong and Kastesz[18] and closely resembles that of polyethylene[16].

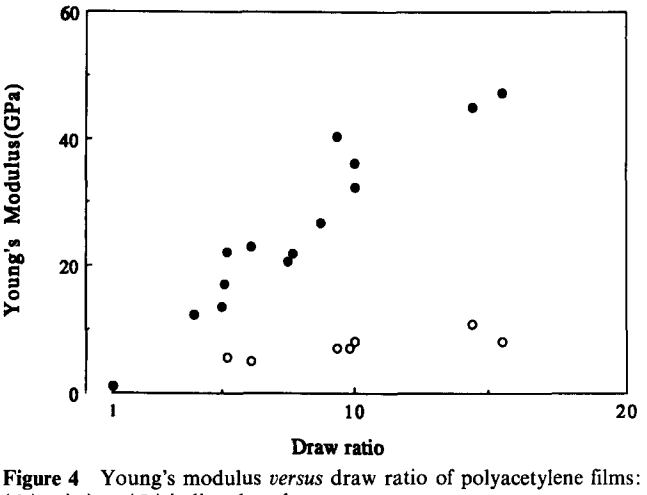

Figure 4 Young's modulus *versus* draw ratio of polyacetylene films: (●) pristine; (○) iodine-doped

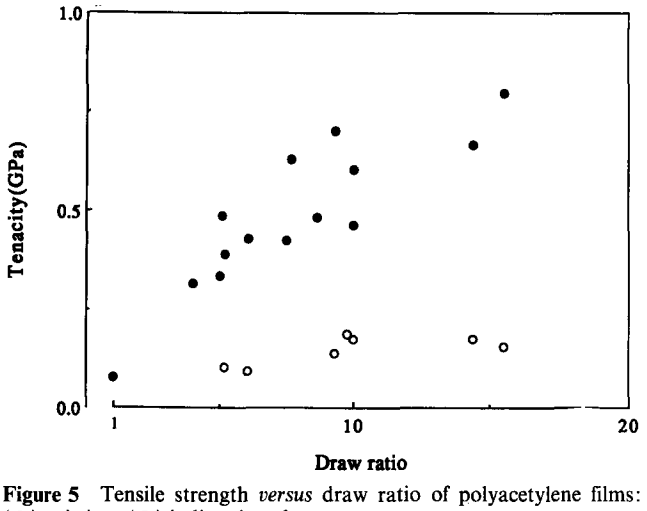

Figure 5 Tensile strength *versus* draw ratio of polyacetylene films: (●) pristine; (○) iodine-doped

Typical load–elongation curves for both undoped and doped polyacetylene films drawn to $\lambda = 14.4$ are shown in *Figure 7*. This figure reveals that the slope of the load–elongation curve decreased by about a factor of 2 on doping into the metallic regime, indicating a substantial decrease in the stiffness. The reduction in the stiffness is even more pronounced because the cross-sectional area of the film increased by about a factor of 2 on doping.

Thus, taking into account the effect of volume expansion upon doping, the Young's modulus decreased by about a factor of 4–5. Values of the modulus and tensile strength *versus* draw ratio of polyacetylene *doped* to maximum conductivity (see below) are plotted in *Figures 4* and *5*, for comparison with the corresponding properties of the undoped samples. Both the modulus and tenacity consistently decreased by about a factor of 4–5.

It is not surprising to find some degradation of the mechanical properties after doping; this is to be expected when the mechanical properties are limited by the relatively weak secondary interactions (for conjugated polymers, the interchain electron transfer interaction and van der Waals bonds). The observed decreases in modulus and tenacity after doping imply an associated reduction in the interchain electronic coupling. This reduction presumably arises because of the intercalation of the counterions (columns or sheets, etc.) into the structure.

In *Table 3*, we compare the mechanical properties of polyacetylene doped by different methods and with different counterions. Of the three different dopant counterions, I_3-doped materials retain the maximum mechanical properties by a considerable margin (note also that in the case of iodine, the films were doped to maximum levels, while for $FeCl_3$ and $NOSbF_6$ the doping levels were moderate).

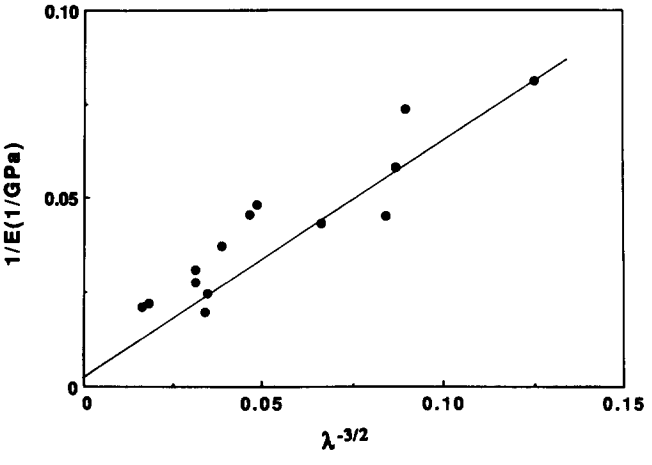

Figure 6 E^{-1} *versus* $\lambda^{-3/2}$ in comparison with equation (2)

Electrical conductivity

Figure 8 shows the correlation between the electrical conductivity and the draw ratio (λ) for both thick ($\sim$25–30 μm, after tensile drawing) and thin ($\sim$3–5 μm, after drawing) iodine-doped polyacetylene films prepared as described above. The conductivity was found to increase essentially linearly with the draw ratio: the maximum conductivity was 2×10^4 S cm^{-1} at a draw ratio of $\lambda = 15$ for the thick films, and 3×10^4 S cm^{-1} at a draw ratio of $\lambda = 10$ for thin films. The slope of σ *versus* λ for thin films is approximately a factor of 2 greater

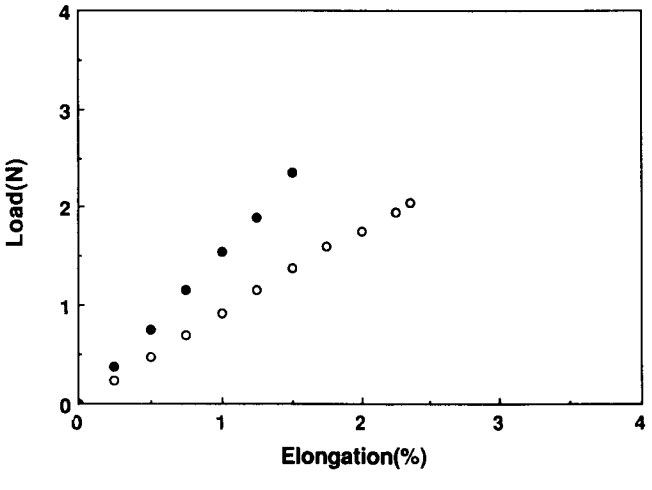

Figure 7 Load *versus* elongation curves for (●) pristine and (○) iodine-doped polyacetylene films ($\lambda = 14.4$)

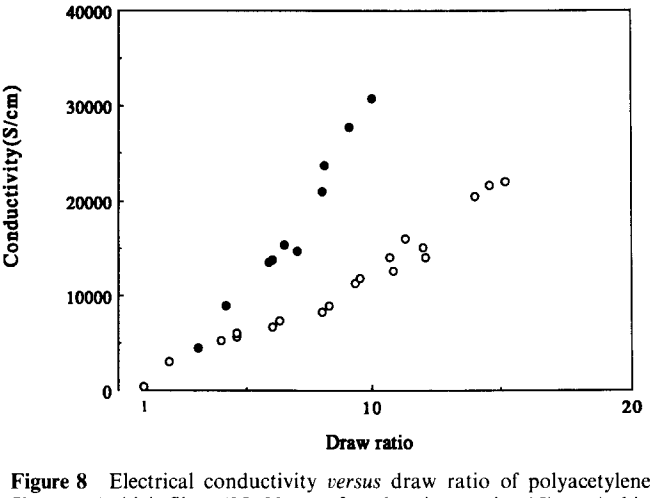

Figure 8 Electrical conductivity *versus* draw ratio of polyacetylene films: (○) thick films (25–30 μm after drawing to $\lambda = 15$); (●) thin films (3–5 μm after drawing to $\lambda = 10$)

Table 3 Mechanical properties of doped polyacetylene, $[(CH)^{y+}A_y^-]_x$

Dopant	Initial draw ratio	y	Tenacity (GPa)	Modulus (GPa)	Elongation (%)	σ (S cm^{-1})
Pristine	10.0	0	0.60	36.2	1.0	
	7.5	0	0.43	20.7	1.0	
I_2[a]	10.0	0.27	0.19	7.1	1.3	1.3×10^4
	7.5	0.27	0.13	5.0	1.8	8.6×10^3
$FeCl_3$[b]	10.0	0.03	0.16	5.8	3.8	9.8×10^3
	7.5	0.03	0.20	5.5	5.6	7.9×10^3
$NOSbF_6$[b]	10.0	0.06	0.05	1.49	5.8	3.0×10^3
	7.5	0.055	0.07	0.81	9.2	1.3×10^3

[a]Doping in gas phase
[b]Doping in nitromethane solution

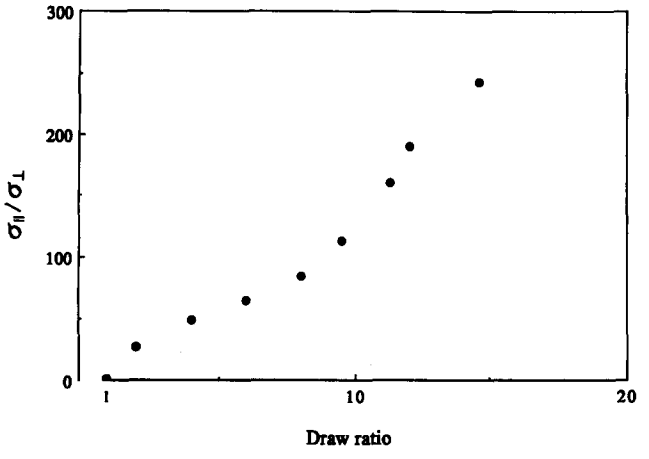

Figure 9 Anisotropy of the electrical conductivity *versus* draw ratio of doped polyacetylene films

than that of thick films (a significant thickness dependence of the conductivity is consistent with the results described in the recent report of Kasai *et al.*[19]). The data imply that, if more homogeneous thin films can be prepared and stretched to higher draw ratios, higher conductivities may be possible.

We have no specific microscopic information on the differences between the thin and thick films; evidently the details of the polyacetylene polymerization (see above) and/or doping result in higher-quality material for the thin films. The conclusion, however, is unambiguous; thin films may have fewer structural defects (e.g. sp^3 carbons), higher molecular weight (or both), or they might be more homogeneously doped.

Figure 9 shows the anisotropy of electrical conductivity *versus* draw ratio. The anisotropy increased with increasing draw ratio, reaching $\sigma_{\parallel}/\sigma_{\perp} \approx 250$ as $\lambda \rightarrow 15$. Although the parallel conductivity increased dramatically as a function of the draw ratio, the conductivity perpendicular to the tensile drawing direction was essentially constant with increasing draw ratio (for $\lambda \geqslant 2$). These data set a lower limit on the anisotropy of the intrinsic conductivity of oriented polyacetylene. The results imply that heavily doped polyacetylene is a quasi-one-dimensional 'metal' with relatively weak interchain coupling.

Doping by $FeCl_3$ or $NOSbF_6$ in CH_3NO_2 solution always gave lower conductivities. Typical values are summarized in *Table 3*, together with their mechanical properties. The electrical conductivity data are thus consistent with the degree of structural order and chain alignment as inferred from the X-ray diffraction data. Whether or not the one-dimensional channel structure inferred for the I_3-counterions plays an important role is a subject worthy of more detailed study.

Correlation between electrical conductivity and mechanical properties

Figures 10 and *11* demonstrate a direct correlation between the electrical conductivity and the mechanical properties (Young's modulus and tenacity, respectively) of polyacetylene. The linear relationship implies that the increase in the electrical conductivity with increasing draw ratio must result from increased uniaxial orientation, improved lateral packing and associated enhanced interchain interaction, as is the case for the mechanical properties. Moreover, the correlation between mechanical and electrical properties demonstrated in *Figures 10* and *11* (as a function of draw ratio for I_3-counterions) is evident in *Table 3*, where the different dopants are compared.

The reduction of the modulus and tenacity after doping is consistent with the large anisotropy in the electrical conductivity; the quasi-one-dimensionality implies relatively weak interchain coupling. The reduced interchain electronic coupling implies an associated reduction in the electronic energy bandwidth in the transverse direction.

Although the electrical conductivity of conducting polymers is enhanced by the relatively high mobility associated with intrachain transport, one must have the possibility of interchain charge transfer to avoid the localization inherent to one-dimensional electronic systems[20,21]. The electrical transport becomes three-dimensional (and thereby truly metallic) so long as there is a high probability that an electron will have diffused to a neighbouring chain between defects on a single chain. For well ordered crystalline material in which the chains have precise phase order, the interchain diffusion is a coherent process. In this case, the condition for extended anisotropic transport is that[20,21]:

$$L/a \gg t_0/t_{3d} \tag{3}$$

where L is the coherence length, a is the chain repeat unit length, t_0 is the intrachain π-electron transfer

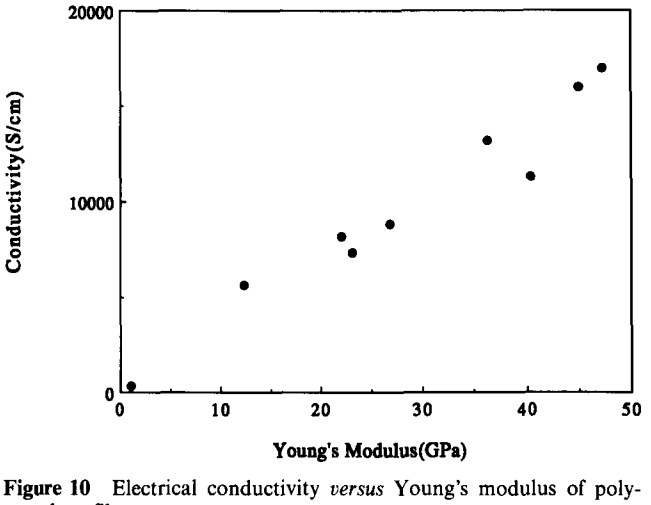

Figure 10 Electrical conductivity *versus* Young's modulus of polyacetylene films

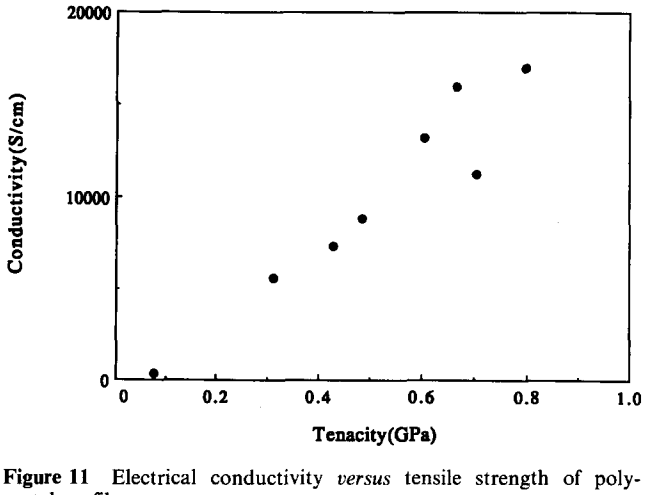

Figure 11 Electrical conductivity *versus* tensile strength of polyacetylene films

integral, and t_{3d} is the interchain π-electron transfer integral. An analogous argument can be constructed for achieving the intrinsic strength of a polymer, i.e. the strength of the main-chain covalent bonds. If E_0 is the energy required to break the covalent main-chain bond and E_{3d} is the weaker interchain bonding energy (from van der Waals forces and hydrogen bonding for saturated polymers), then the requirement is coherence over a length L such that[21,22]:

$$L/a \gg E_0/E_{3d} \tag{4}$$

In this limit, the large number (L/a) of weak interchain bonds add coherently such that the polymer fails by breaking the covalent bond. The direct analogy between inequalities (3) and (4) is evident. In fact, for conjugated polymers, E_0 results from a combination of σ and π bonds (the latter being equal to t_0; see equation (2)) and E_{3d} is dominated by the interchain transfer integral, t_{3d}. Thus, the inequalities (3) and (4) imply that, quite generally, the conductivity and the mechanical properties will improve in a correlated manner as the degree of chain alignment is increased. This prediction is in excellent agreement with the data obtained from polyacetylene, as shown in *Figures 10* and *11*.

Assuming that the linear correlation of *Figures 10* and *11* persists to even higher draw ratios, the extrapolated modulus of 300 GPa (see *Figure 6*) would imply that the electrical conductivity for perfectly oriented polyacetylene prepared as described above would be approximately 2×10^5 S cm^{-1}. However, this extrapolated value may still be limited by structural defects (e.g. sp^3 defects, etc.) rather than by intrinsic phonon scattering. In this context, we note once again that, prior to any tensile drawing, the value for the conductivity of our samples was about 500 S cm^{-1}, whereas considerably higher values have been reported[3,23]. Thus, we envision a series of curves like those shown in *Figures 10* and *11*, but with slopes that increase with sample perfection until the mean free path becomes limited by phonon scattering. A theoretical estimate[20] of the intrinsic conductivity (limited by phonon scattering) at room temperature is 2×10^6 S cm^{-1}, an order of magnitude greater than that inferred from the extrapolation of *Figures 6* and *10*.

CONCLUSIONS

We have found that the maximum draw ratio of polyacetylene films prepared by non-solvent polymerization can be significantly improved by using appropriate organic liquids as plasticizers; draw ratios up to 15 have been achieved.

The wide-angle X-ray diffraction patterns of these films demonstrate a high degree of preferred orientation of the crystalline lattice along the drawing axis. Linewidths of the principal equatorial reflections imply long-range order in the chain packing with a lateral coherence length of approximately 20 nm. The structural coherence length increased somewhat (from approximately 10 nm at $\lambda = 4$ to approximately 20 nm at $\lambda = 15$) with tensile drawing, thereby demonstrating on the molecular scale the positive effect of post-synthesis processing of polyacetylene (in contrast to simple fibrillar alignment). Upon doping, diffraction features appeared on the meridian, which indicated the formation of a sublattice of the counterions. For iodine doping, the I_3-counterions appear to be arranged in columns in 1d channels between the polyacetylene chains, with almost no phase coherence from column to column.

The mechanical properties (Young's modulus and tensile strength) were found to increase with increasing draw ratio. At a draw ratio of 15, the modulus and tenacity were 50 GPa and 0.9 GPa, respectively, for undoped polyacetylene, i.e. comparable with the values obtained for ultra-high-molecular-weight polyethylene drawn to the same draw ratio. Based on analysis of the data as a function of the draw ratio, the Young's modulus for perfectly oriented polyacetylene films was estimated to be approximately 290 GPa.

Doping decreases both Young's modulus and the tenacity by a factor of approximately 4. Since (at least in the case of iodine doping) the degree of chain alignment remains essentially unchanged, the reduced mechanical properties are attributed to a decrease in the magnitude of the interchain electron transfer interaction. This evidence of reduced interchain coupling is consistent with the large value found for the anisotropy in the electrical conductivity; at the maximum draw ratio, $\sigma_{\parallel}/\sigma_{\perp} > 250$.

The oriented polyacetylene films prepared in this study exhibit electrical conductivities as high as 2.0×10^4 S cm^{-1} for thick films (25–30 μm) at a draw ratio of 15, and 3.0×10^4 S cm^{-1} for thin films (3–5 μm) at a draw ratio of 10 (measured parallel to the stretching direction after doping with iodine in the gas phase).

A direct, linear correlation between the electrical conductivity and the mechanical properties (Young's modulus and tenacity) of polyacetylene has been demonstrated. In general for polymers, the modulus and tensile strength derive from a combination of the intrachain interactions (e.g. strength of chemical bonding, chain conformation, etc.) and interchain interaction (e.g. van der Waals forces, interchain transfer interactions, chain conformation, etc.)[22]. In conjugated polymers, these same features (band conduction within a polymer chain and efficient electron transfer between polymer chains) determine the carrier mean free path, and thus the electrical conductivity. We conclude, therefore, that the mechanical and electrical properties of doped conjugated polymers are intrinsically linked, and we anticipate that in general, as the tensile strength (and/or modulus) improve with improved chain orientation, the electrical conductivity will show corresponding improvements until both approach their respective intrinsic theoretical values.

ACKNOWLEDGEMENTS

This research was supported by the Electric Power Research Institute (EPRI grant RP8007-9). The authors are deeply indebted to Professor H. Shirakawa for many helpful discussions on the non-solvent method of polyacetylene preparation and for sharing his data on the mechanical properties.

REFERENCES

1 Chiang, C. K., Fisher, C. R. Jr, Park, Y. W., Heeger, A. J., Shirakawa, H., Louis, E. J., Gau, S. C. and MacDiarmid, A. G. *Phys. Rev. Lett.* 1977, **39**, 1098

2 Lugli, G., Pedretti, U. and Perego, G. *J. Polym. Sci., Polym. Lett. Edn* 1985, **213**, 129

3 Naarmann, H. *Synth. Met.* 1987, **17**, 223; Naarmann, H. and Theophilou, N. *Synth. Met.* 1987, **22**, 1

4 Akagi, K., Suezaki, M., Shirakawa, H., Kyotani, H., Shimamura, M. and Tanabe, Y. *Synth. Met.* 1989, **28**, D1
5 Kyotani, H., Shimamura, M., Tanabe, Y., Watanabe, Y., Suezaki, M., Kasai, T., Akagi, K. and Shirakawa, H. *Rep. Prog. Polym. Phys. Japan* 1988, **31**, 265
6 Shirakawa, H. and Ikeda, S. *Synth. Met.* 1979/1980, **1**, 175
7 Bradley, D. D. C., Frienol, R. H., Hartmann, T., Marseglia, E. A., Sokolowski, M. M. and Townsend, P. D. *Synth. Met.* 1987, **17**, 473
8 Montaner, A., Rolland, M., Sauvajol, J. L., Galtier, M., Almairac, R. and Ribet, J. L. *Polymer* 1988, **28**, 1101
9 Pouget, J. P. *Solid State Sci.* 1985, **63**, 26
10 Winokur, M., Moon, Y. B., Heeger, A. J., Barker, J., Bott, D. C. and Shirakawa, H. *Phys. Rev. Lett.* 1987, **58**, 2329
11 Baughman, R. H., Murthy, N. S., Miller, G. G. and Shacklette, L. W. *J. Chem. Phys.* 1983, **79**, 1065
12 Monkenbusch, M., Murra, B. S. and Wegner, G. *Makromol. Chem., Rapid Commun.* 1982, **3**, 69
13 Shimamura, K., Yamashita, Y., Kasahara, H. and Monobe, K. *Synth. Met.* 1987, **17**, 485
14 Wiener, G., Weizenhoter, R., Monkenbusch, M., Stamm, M., Leiser, G., Enkelmann, V. and Wegner, G. *Makromol. Chem., Rapid Commun.* 1985, **5**, 425
15 Smith, P. and Lemstra, P. J. *J. Mater. Sci.* 1980, **15**, 505
16 Irvine, P. A. and Smith, P. *Macromolecules* 1986, **19**, 240
17 Shimamura, M., Kyotani, H., Tanabe, Y., Agaki, K., Suezaki, M., Kasai, T. and Shirakawa, H. *Polym. Prepr. Japan* 1989, **38**, 967
18 Hong, S. Y. and Kertesz, M. preprint
19 Kasai, T., Zhang, Y., Akagi, K. and Shirakawa, H. *Polym. Prepr. Japan* 1989, **38**, 2111
20 Kiverson, S. and Heeger, A. J. *Synth. Met.* 1988, **22**, 371
21 Heeger, A. J. *Faraday Discuss., Chem. Soc.* 1989, **88**, 1
22 Termonia, Y. and Smith, P. in 'The Path to High Modulus Polymers with Stiff and Flexible Chains' (Eds A. E. Zachariades and R. S. Porter), Marcel Dekker, New York, 1988, p. 321
23 Tsukamoto, J., Takahashi, A. and Kawasaki, K. *Japan. J. Appl. Phys.* 1990, **29**, 1